

Measuring the spin up of the Accreting Millisecond Pulsar XTE J1751–305

A. Papitto^{1,2*}, M.T.Menna², L.Burderi³, T.Di Salvo⁴, and A.Riggio³

¹*Dipartimento di Fisica, Università degli Studi di Roma "Tor Vergata", via della Ricerca Scientifica 1, 00133 Roma, Italy*

²*Osservatorio Astronomico di Roma, via Frascati 33, Monteporzio Catone, 00040, Italy*

³*Dipartimento di Fisica, Università degli Studi di Cagliari, SP Monserrato-Sestu, KM 0.7, Monserrato, 09042 Italy*

⁴*Dipartimento di Scienze Fisiche ed Astronomiche, Università di Palermo, via Archirafi 36, Palermo, 90123, Italy*

3 December 2021

ABSTRACT

We perform a timing analysis on RXTE data of the accreting millisecond pulsar XTE J1751–305 observed during the April 2002 outburst. After having corrected for Doppler effects on the pulse phases due to the orbital motion of the source, we performed a timing analysis on the phase delays, which gives, for the first time for this source, an estimate of the average spin frequency derivative $\langle \dot{\nu} \rangle = (3.7 \pm 1.0) \times 10^{-13}$ Hz/s. We discuss the torque resulting from the spin-up of the neutron star deriving a dynamical estimate of the mass accretion rate and comparing it with the one obtained from X-ray flux. Constraints on the distance to the source are discussed, leading to a lower limit of ~ 6.7 kpc.

Key words: stars: neutron – stars: magnetic fields – pulsars: general – pulsars: individual: XTE J1751–305 – X-ray: binaries

1 INTRODUCTION

Accreting millisecond pulsars (AMSP in the following) are the long sought connection between low mass X-ray binaries (LMXBs) and millisecond radio pulsars. In fact, although it was hypothesised soon after their discovery that fast spinning radio pulsars were “recycled” by an accretion phase in a LMXB system, during which the neutron star (NS) is spun-up (see for a review Bhattacharya & van den Heuvel 1991), evidence has been elusive since SAX J1808.4–3658, the first accretion-driven millisecond X-ray pulsar, was discovered (Wijnands & van der Klis 1998). SAX J1808.4–3658, with a spin period of 2.5 ms, exhibiting both X-ray bursts and coherent pulsations, proved to be the missing link between the two classes of sources. Since then, six more millisecond X-ray pulsars were discovered (see Wijnands 2006 for an observational review).

All of these sources are transients with usually low duty cycles. Except for the case of HETE J1900.1–2455 which remained active for more than a year after its discovery in June 2005 (Galloway et al. 2007), the outbursts of AMSP last for no more than a couple of months, with recurrence times usually larger than 2 yr (Galloway 2006). Although the sample is still small, monitoring of future outbursts exhibited by the known sources is extremely important for our understanding of LMXBs and their evolution.

The study of the rotational behaviour of these sources during outbursts is on the other hand obviously fundamental as a test of theories of accretion physics. As a matter of fact, the measure of the variations of the spin frequency gives immediate understanding of the torques experienced by the compact object because of the accretion of matter, and further allows a model dependent dynamical estimate of the instantaneous mass accretion rate. Timing techniques performed on the coherently pulsed emission (see e.g. Blandford & Teukolsky 1976) represent the key tool in order to directly measure the variations of the spin rate of this kind of accretors. The application of this kind of analyses on the X-ray emission of these sources, as observed by the high temporal resolution satellite Rossi X-Ray Timing Explorer (*RXTE*) (Bradt et al. 1983), allowed the measurement of the spin frequency derivative in the case of IGR J00291+5934 (Falanga et al. 2005; Burderi et al. 2007), XTE J0929–314 (Galloway et al. 2002), XTE J1814–338 (Papitto et al. 2007), XTE J1807–294 (Riggio et al. 2007) and of one of the outbursts shown by SAX J1808.4–3658 (Burderi et al. 2006). See Di Salvo et al. (2007) and references therein for a review.

Even though the shortness of the outbursts generally exhibited by AMSP strongly limits the capability of the timing analysis in discriminating between various accretion models, observations have already shown how the behaviour of these sources can be variable, in fact, as a result of accretion, some of them are observed to spin up, while others decelerate. In this work we present a timing analysis performed on the only

* E-mail: papitto@oa-roma.inaf.it

outburst of XTE J1751–305 observed so far by *RXTE* with its highest temporal resolution mode, and discuss the observed spin frequency evolution as a result of the accretion torques acting on the NS. Moreover the measure of the spin frequency derivative is used to infer a dynamical estimate of the peak mass accretion rate during the outburst, which can be compared with the estimate deduced from spectral modelling of the X-ray emission, in order to give an estimate of the distance to the source.

2 OBSERVATIONS AND DATA ANALYSIS

XTE J1751–305 was first detected monitoring the Galactic bulge region with the Proportional Counter Array (PCA) on board the *RXTE* (Markwardt & Swank 2002a). Subsequently, pointed observations in April 2002, allowed the detection of an X-ray periodic modulation at a frequency of about 435 Hz, establishing that this source belongs to the class of accreting millisecond X-ray pulsars (Markwardt et al. 2002b, M02 hereafter). Throughout this paper we used a sample of *RXTE* public domain data taken between 4 and 30 April 2002. The data we use to perform the timing analysis are those collected by the Proportional Counter Array (PCA, Jahoda et al. 1996), which is made by five units (PCUs) sensitive in the 2 – 60 keV band, for an overall collecting area of ~ 6250 cm². Except the observations of April 4, which were taken in Good Xenon configuration with a $1\mu\text{s}$ time resolution (2 s read out time and 256 energy channels), all the other PCA data we considered are Generic Event (E_125us_64M_0.1s) with a temporal resolution of $122\mu\text{s}$ and 64 energy channels. All the data were processed and analysed using the HEASARC FTOOLS v.6.0.

The source was first spotted by the PCA in the desired collecting mode at $T_0 = 52368.653$ MJD, which represents the start time of observations throughout this paper. Thereafter the X-ray light curve of XTE J1751–305 is made of two exponential decays with different e-folding factors. The first one describes the first 8.5 d of observation and can be modelled with the function $L_X(t) = L_X(\bar{T})\exp[-(t - \bar{T})/\tau_d^{(1)}]$, where $L_X(\bar{T})$ is the luminosity at $\bar{T} = 52369.644$ MJD and $\tau_d^{(1)} = 7.2$ d (see Gierlinski & Poutanen (2005), GP hereinafter, for the 2 – 20 keV light curve; see also M02). Subsequently the light curve experiences a sharp break and can be described with a similar decay function this time with $\tau_d^{(2)} = 0.63$ d. The source then switches back to the quiescence emission levels, ~ 10 d after the first available observation. Considering a physically motivated spectral model (see the discussion for further details) GP estimated for the bolometric X-ray/ γ -ray luminosity attained by XTE J1751–305 during the outburst $L_X(\bar{T}) = 2.7 \times 10^{37} d_{8.5}^2 \text{ erg s}^{-1}$, where $d_{8.5}$ is the distance to the source in units of 8.5 kpc.

The technique we used in order to perform the timing analysis on the pulsed emission is extensively described in Burderi et al. (2007, see also Papitto et al. 2007). We first corrected X-ray photons arrival times to the Solar system barycentre considering the best position available for this source from Chandra (M02). We then focused on the orbital modulation of the phases to derive an accurate orbital solution. The evolution of the phases, measured by folding 90 s long intervals around the M02 estimate of the spin period, was modelled with Eq.1 of Papitto et al. (2007), without

Table 1. Orbital and timing parameters of XTE J1751–305

	M02	This work ^a
Orbital solution		
$a \sin i/c$ (lt-ms)	10.1134(83)	10.125(5)
P_{orb} (s)	2545.3414(38)	2545.342(2)
T^* (MJD)	52368.0128983(87) ^b	52368.0129023(4)
Eccentricity e	$< 1.7 \times 10^{-3}$	$< 1.3 \times 10^{-3}$
Timing Solution		
ν_0 (Hz)	435.317993681(12)	435.31799357(4)
$< \dot{\nu} >$ (Hz/s)	$< 3 \times 10^{-13}$ ^c	$(3.7 \pm 1.0) \times 10^{-13}$.
$\dot{\nu}(\bar{T})$ (Hz/s) $\alpha = 2/7$		$(5.6 \pm 1.2) \times 10^{-13}$

^a Numbers in parentheses, referring to our values, are the 90% confidence level uncertainties in the last significant figure, while the ones referring to M02 are given at 3σ confidence level on the last significant digits. The same confidence levels are considered in giving upper limits on the eccentricity, e .

^b The value reported here is revised with respect to the one originally quoted in M02 (Markwardt et al. 2007).

^c This upper limit is to be considered on the absolute value of $< \dot{\nu} >$.

considering the term owing to the position uncertainties (see below). The orbital parameters we obtain, namely the projected semi-major axis measured in light ms, $a \sin i/c$, the orbital period, P_{orb} , the time of passage of the NS at the ascending node of the orbit, T^* , and the eccentricity, e , are listed in Tab.1, which contains for comparison purposes also the ones reported by M02. The two orbital solutions are in good agreement within the quoted uncertainties.

The times of arrival of X-ray photons were then reported to the line of nodes of the binary system orbit considering our orbital solution. As the time over which any uncertainty on the orbital parameters may possibly affect the phases of the X-ray pulsations (P_{orb}) is much smaller than the time required for the spin frequency derivative to produce a significant effect, the two effects on residuals can be decoupled. The effect on pulse phases due to the remaining uncertainty on the orbital parameters, $\sigma_{\phi orb}$, can therefore be treated as a normally distributed source of error (see Eq.3 of Burderi et al. 2007 for an expression of $\sigma_{\phi orb}$). The final uncertainty, σ_{ϕ} , on the phase residuals we consider in the following is then the squared sum between $\sigma_{\phi orb}$ and the statistical error arising from sinusoidal fitting of the pulse profiles.

By folding each light curve corrected for the orbital motion of the system around our guess for the spin frequency ν_F (which initially was the M02 estimate), we could detect coherent pulsations until MJD 52377.6, 9 d after the first observation available, when the X-ray flux had become approximately one tenth of the peak flux.

The criterion we considered in order to assess the presence of a periodic signal is simply based on the expected statistic distribution followed by a folded light curve in which no signal is present (Leahy et al. 1983). The statistics S used to check the presence of a periodic signal is defined

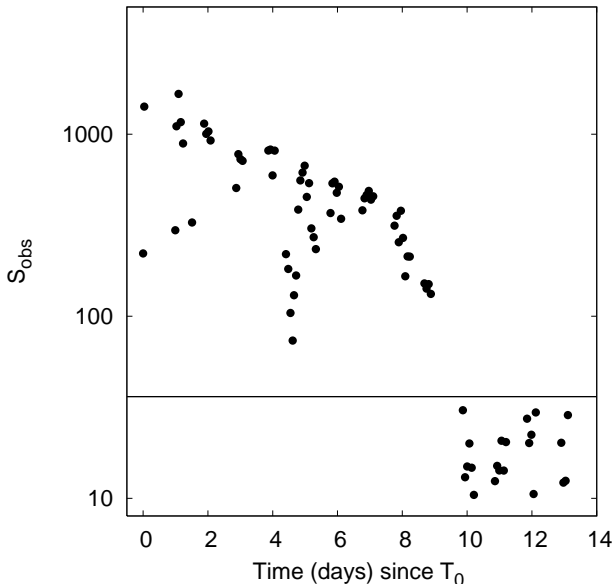


Figure 1. Plot of the observed statistics S_{obs} of every considered folded light curve. The horizontal line represents the 99% confidence limit for the detection of pulsations.

as

$$S = \sum_{j=1}^n \frac{(R_j - R)^2}{\sigma^2}, \quad (1)$$

where n is the number of phase bin by which the light curve is divided, $j = 1, \dots, n$, R_j is the count rate in the j -th bin, R is the average count rate in the considered observation, and $\sigma^2 = R \times n/T$, with T total time of integration. It is assumed that in the absence of periodicity the photon counting in each bin of a folded light curve, $R_j \times T/n$, is pure Poissonian counting noise, so that its mean and variance can be estimated from the average number of counts in each bin, $R \times T/n$. In the limit of a large number of counts, as in the case of the 2002 outburst of XTE J1751–305, when $R \times T/n \gtrsim 2000$, we can assume that this distribution behaves as a Gaussian with the mean equal to the variance. If these conditions are met the statistic S of a folded light curve with no signal is expected to follow a chi-squared distribution with $n - 1$ degrees of freedom. It is then immediate to define a threshold for the detection of the signal S_0 from the desired confidence level P , $(1 - P/100) = Q_{n-1}(\chi_0^2 = S_0)$, where the term on the right hand side is the integrated probability from χ_0^2 to ∞ of a chi-squared distribution with $n - 1$ degrees of freedom. In this case we chose $P = 99$ and $n = 19$, so that every observation with $S_{obs} < 36.19$ was considered as containing no signal at the considered level of significance, and therefore withdrawn from the sample used in timing analysis (see Fig.1).

Folded light curves that met the detection criterion were then modelled with a sinusoid with the period fixed to the folding one. We also tried to add an harmonic to the fitting function, but such a component was significantly detected and led to a slightly better quality fit only in a small fraction of the observations ($\leq 10\%$), so that we consider for the purposes of the timing analysis only the phases obtained with a single harmonic sinusoidal function. An example of the pulse profile is shown in Fig.2.

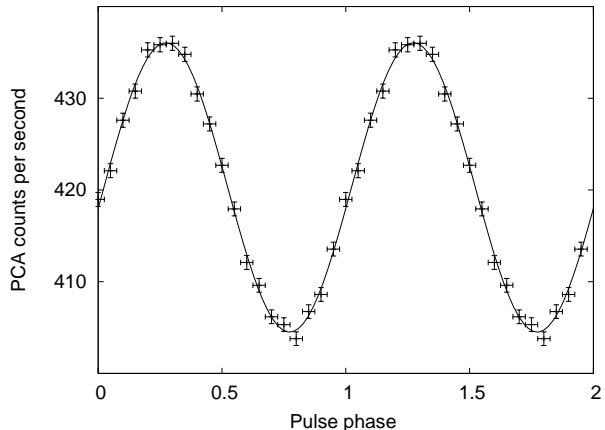


Figure 2. Pulse profile produced folding in 20 phase bins around $\nu_0 = 435.31799357$ Hz, all the available observations spanning the time interval from MJD 52370.537 to MJD 52370.776 (OBSID 70131-01-02-00). This time interval does not represent a continuous time series and the effective total integration time is $\simeq 14$ ks. The solid line is the best fitting sinusoid. The reduced chi squared of this model is $\chi_r^2 = 0.78$ and is not significantly improved by adding an harmonic. Two cycles are plotted for clarity.

Therefore we modelled phase residuals with a parabolic function

$$\Delta\Phi(t) = 1/\nu_F \times (\delta + \beta t + \gamma t^2), \quad (2)$$

where ν_F is the folding frequency, $\beta = -\Delta\nu_0$ is the correction to ν_F to obtain an estimate of the spin frequency at $t = T_0$, $\gamma = -\langle \dot{\nu} \rangle / 2$ is the term owing to a constant spin frequency derivative and δ is a phase constant. This procedure was repeated several times, correcting each time the frequency over which we fold the light curves, until the linear term of Eq.2 was compatible with being null within the uncertainties. The timing parameters we finally obtain are $\nu_0 = 435.31799357(3)$ Hz and $\langle \dot{\nu} \rangle = 3.7(8) \times 10^{-13}$ Hz/s, where the numbers in parentheses are the 90% confidence level uncertainties on the last significant figure, as for all the uncertainties quoted in the rest of the paper.

In Fig.3 we plot the phase delays $\Delta\Phi(t)$, measured in microseconds, of light curves folded around ν_0 , versus the time elapsed since the first observation considered. The plotted error bars refer to the overall 1σ uncertainties on phases, computed by considering both the statistical errors coming from the sinusoidal modelling and the errors induced by the uncertainties on the orbital parameters listed in the right column of Tab.1, as already stated. The reduced chi squared of the quadratic best fitting model is 81/56, which compared to the one obtained with a linear fit (136/57), gives an F test probability of 8×10^{-8} that the improvement in the variance is purely given by chance.

As already shown for other sources of this class (Burderi et al. 2006, Papitto et al. 2007, Riggio et al. 2007) the presence of timing noise, probably due to changes in the position of the emitting hot spot on the NS surface, suggests caution in considering the reliability of the uncertainties on the timing parameters obtained by a simple least square fit to the phase residuals, taken with their uncertainties σ_ϕ . Nevertheless the pulse phase evolution of XTE J1751–305 can be modelled satisfactorily by a general parabolic trend (see

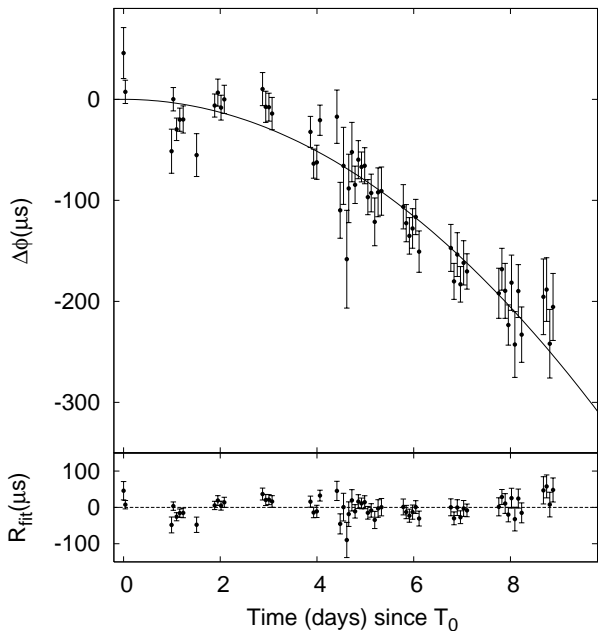


Figure 3. Evolution of the pulse phase delays, measured in microseconds, folding every available observation around $\nu_0 = 435.31799357$ Hz. The plotted error bars are the 1σ uncertainties on phases, including both the statistical errors from the pulse profile sinusoidal fitting and the errors induced by the residual uncertainties on orbital parameters. We note that these error bars have not been rescaled by the factor 1.2 that makes $\chi_r^2 = 1$, which we used to get the errors in the parameters given in Tab.1 (see text for details). The solid line is the best fit constant $\dot{\nu}$ model (upper panel). Residuals with respect to the best-fitting model (lower panel).

Discussion for a comparison with the behaviour displayed by other sources of this class), even if the presence of small timing residuals leads to a reduced χ^2 slightly higher than one. Therefore, in order to get a conservative estimate of the uncertainties affecting the measured spin frequency and its derivative, we amplified all the errors on our phase measurements by a common factor (1.2) until we obtain $\chi_r^2 = 1$ from a fit with Eq.2. We then consider as the most conservative the uncertainties σ_{ν_0} and $\sigma_{\dot{\nu}}$ so obtained. In this way we get to our final estimates of the timing parameters, which are the ones listed in Tab.1. For sake of clarity we note however that the error bars plotted in Fig.3 are not multiplied by any factor and they represent the genuine 1σ uncertainties on the measured phases.

A more physically motivated description of the evolution of phase delays is easily obtained if the dependency of $\dot{\nu}(t)$ on the accretion rate is considered. According to the simplest model of angular momentum exchange between the accreting matter and the compact object, matter in the disc can be considered fully diamagnetic, so that the only relevant torque is the positive one coming from accretion of matter at the inner boundary of the disc, which is placed at a distance R_{in} from the centre of the compact object. In an X-ray pulsar this boundary can be determined, at least by orders of magnitude, considering the balance between the ram pressure of the infalling matter and the magnetic pressure of the field that truncates the disc. When mass

accretion rate declines, as in the fading parts of the outburst light curves of X-ray transients like XTE J1751–305, the pressure of falling matter is expected to decrease letting the magnetosphere to expand. Assuming that the inner disc boundary scales as $R_{in} \propto \dot{M}^{-\alpha}$, with $\alpha \geq 0$ and constant at every experienced accretion rate, the integral of the spin up torque exerted by matter accreting at R_{in} can be therefore carried on in terms of the instantaneous value of the mass accretion rate. The instantaneous spin frequency derivative can then be expressed as (see e.g. Burderi et al. 2007):

$$\dot{\nu}(t) = \frac{1}{2\pi I} l_0 \dot{M}(\bar{t}) \left(\frac{\dot{M}(t)}{\dot{M}(\bar{t})} \right)^{1-\alpha/2}, \quad (3)$$

where $l_0 = (GM R_{in}(\bar{t}))^{1/2}$ is the specific angular momentum of accreting matter evaluated at $t = \bar{t}$. Once it is assumed that $\dot{M}(t) \propto L_X(t)$, the temporal dependence of $\dot{\nu}(t)$ can be expressed in terms of the particular shape of the outburst light curve. As our aim is to compare our estimate of the accretion rate needed to explain the observed $\dot{\nu}$ assuming a certain torque model, and the accretion rate deduced from spectral fitting, we consider here and in the following $\bar{t} = \bar{T}$, an instant for which GP produce an accurate estimate of the 0.7 – 200 keV flux.

Considering an X-ray light curve shape composed only by a single exponential decay, the expected behaviour of the phase delays time evolution is then:

$$\Delta\Phi(t) = \frac{1}{\nu_F} \left\{ A - [B + k\tau_\alpha C] (t - T_0) - C\tau_\alpha^2 \exp\left[-\frac{t - \bar{T}}{\tau_\alpha}\right] \right\}, \quad (4)$$

where $\tau_\alpha = \tau_d(1 - \alpha/2)^{-1}$, τ_d is the e-folding factor of the light curve exponential decay, $k = \exp[-(T_0 - \bar{T})/\tau_\alpha]$, A is a phase constant, $B = \Delta\nu_0$ is the correction to the folded spin frequency and $C = \dot{\nu}(\bar{T}) = (2\pi I)^{-1} [GM R_{in}(\bar{T})]^{1/2} \dot{M}(\bar{T})$ is the spin frequency derivative at $t = \bar{T}$.

We first considered eq.(4) with $\tau_d = 7.2$ d, and fitted the observed phase delays with various values of α , corresponding to different models of disc-magnetosphere interaction. In particular, the case $\alpha = 0$ corresponds to no dependence of R_{in} on the instantaneous accretion rate and in this case we consider $R_{in} = R_C$ where R_C is the corotation radius defined as the radius at which the Keplerian orbiting matter in the disc exactly corotates with the NS magnetosphere (see e.g. Rappaport et al. 2004). On the other hand, $\alpha = 2/7$ is the Alfvénic value obtained in the approximation of spherical accretion of matter. Unfortunately we succeeded in having no significant improvement in the description of the phase residuals by implementing such torque models, as for example we obtain $\chi_r^2 = 79/56$ when $\alpha = 2/7$ is considered.

We also tried other α plausible values, based on a more realistic treatment of the disc structure at the inner rim, which includes different possible regimes, as gas pressure dominated or radiation pressure dominated SS optically thick disc (respectively $\alpha = 0.25$ and 0.15 for models 1G and 1R in Ghosh 1996 and Psaltis & Chakrabarty 1999). We did not consider any other model that would lead to significantly higher values of α (e.g. two temperature optically thin gas pressure dominated discs), as the maximum value that this parameter can attain is the one that implies a full excursion of R_{in} during the outburst, from the NS radius to the corotation radius, while the source keeps showing pulsations (see discussion). Since in the case of XTE

J1751–305 a coherent signal can be detected as long as the X-ray flux, which is related to the instantaneous mass accretion rate, has declined to one tenth of its maximum value, the constraint $R_{in}(t_{cut})/R_{in}(T_0) = (F_x(t_{cut})/F_x(T_0))^{-\alpha} < R_C/R_{NS}$, where $t_{cut} = T_0 + 9$ d is the time at which the pulsations are cut off, leads to $\alpha < 0.4$ for a $1.4 M_\odot$ NS with a $R_{NS} = 11.1$ km radius. The available statistics nevertheless revealed itself to be too low to discriminate between these models. This is witnessed by the fact that the goodness of the fit and also the value of the spin frequency derivative remain almost the same when different plausible values of α are chosen. In order to give a reference value of $\dot{\nu}(\bar{T})$, the spin frequency derivative at $t = \bar{T}$, we consider the simple Alfvénic case, $\alpha = 2/7$, for which $\dot{\nu}(\bar{T}) = (5.6 \pm 1.0) \times 10^{-13}$ Hz/s. In the same way we operated before, we amplified the actual errors on phases by a common factor until we have $\chi_r^2 = 1$ for the best fitting $\alpha = 2/7$ model, thus obtaining the 90% confidence level uncertainty on $\dot{\nu}(\bar{T})$ listed in Tab.1.

We note that an attempt was also made to model the behaviour of the phase delays in terms of the broken decay effectively observed in the X-ray light curve, rather than considering a single decay taking place throughout the outburst. We thus implemented in Eq.4 the change of the e-folding factor that takes place simultaneously to the break. This attempt anyway led neither to improvements in the quality of the fit nor to variations in the measured parameters for every value of α considered. This is probably due to the shortness of the time interval in which the light curve is described by $\tau_d^{(2)}$ before the pulsations fade away.

We conclude this section by noting that a systematic term due to the uncertainty in the source position has to be considered in order to have a reliable estimate of the uncertainty in the spin frequency as well as in the spin frequency derivative. The best position available has a 90% error circle of $0''.6$ (M02), and following the expression given by Burderi et al. 2007, we estimate the upper limit on the effects of this uncertainty on the value of ν_0 as $\sigma_{sys} \nu_0 < 1 \times 10^{-7}$ Hz, while on $\dot{\nu}(\bar{T})$ as $\sigma_{sys} \dot{\nu} < 0.3 \times 10^{-13}$ Hz/s, which is one order of magnitude smaller than the spin frequency derivative we measure, and smaller than the error on $\langle \dot{\nu} \rangle$ quoted above.

3 DISCUSSION

In the previous section we described the application of different accretion models, referring to different assumption on the disc-magnetosphere interaction and on the particular structure of the inner region of the accretion disc, to the observed evolution of the pulse phases of XTE J1751–305, under the assumption that the curvature observed in the phase delays versus time is indeed a measure of the spin frequency derivative.

The stability of the pulse phase evolution of this source resembles the one shown by IGR J00291+5934 (Burderi et al. 2007) and XTE J0929–314 (Galloway et al. 2007) with a smooth variation along the course of the outburst, witnessed by the small post fit residuals obtained even when a simple constant $\dot{\nu}$ model is used. This behaviour is different from the one analysed in an other subset of sources of this class, namely XTE J1814–338 (Papitto et al. 2007) and XTE J1807–294 (Riggio et al. 2007), where the phases

oscillate around the mean trend clearly anticorrelating with rapid (~ 1 d) X-ray flux variations, and SAX J1808.4–3658 (Burderi et al. 2006), which shows an even more complex behaviour. It has to be noted that for all of the latter at least two harmonics are needed to model adequately the pulse profiles, while, among the sources of the first group, only XTE J0929–314 has a significant harmonic content. In particular the trend followed by the phases of the second harmonic seems more stable than the one of the fundamental (Burderi et al. 2006, Riggio et al. 2007), leading the authors to consider the second harmonic to establish the rotational behaviour of the considered source. A correlation between the phase stability and the two class of AMSPs depicted above seems to arise if it is considered that for the last three the X-ray light curve is somehow complex, showing a variety of features, like re-flares, oscillations around a mean trend and in general variations on time scales of days, and simultaneously the pulse phases deviate from a continuous trend. The light curves of the first three instead generally show a quite smooth exponential decay, during which the phases distribute themselves normally around the mean trend.

A discussion of the noise of AMSP pulse phases around their mean trend is beyond of the scope of this paper, nevertheless these considerations make us even more confident on the stability of the evolution of the pulse phases in the case of XTE J1751–305, a source in which no secondary harmonics appear nor the light curve deviates from an exponential decay through the time interval considered here. We therefore ascribe the parabolic trend followed by the phases to a spin frequency evolution due to the accretion torques acting on the NS when it is efficiently accreting mass.

However the attempts made proved unsuccessful in discriminating a constant spin up model from a model in which the spin frequency derivative depends on the instantaneous value of the mass accretion rate, as traced by the observed X-ray flux. In the hypothesis that $\dot{\nu}(t) \propto \dot{M}(t) \propto F_X(t)$, which we stress is not favoured nor disfavoured by the data, the measurement of the spin frequency derivative of XTE J1751–305 at $t = \bar{T}$, $\dot{\nu}(\bar{T})$, allows a dynamical estimate of the mass accretion rate. This can be further compared with the estimate of the flux observed jointly by *XMM* and *RXTE*, in order to constrain the distance to the source. The evaluation of Eq.(3) at the time $t = \bar{T}$, together with the estimate of $\dot{\nu}(\bar{T})$ given in the previous section, leads to an expression that relates mass accretion rate at that time to the lever arm of the spin up torque at the same time, i.e. the inner disc radius:

$$\dot{M}_0 = (30 \pm 6) \times 10^{-10} I_{45} m^{-2/3} \xi^{-1/2} M_\odot/\text{yr}, \quad (5)$$

where I_{45} is the moment of inertia of the compact object in units of 10^{45} g cm², m is the mass of the NS in solar units, and $\xi = R_{in}/R_C$ is a parametrisation of the inner disc radius at \bar{T} in terms of the corotation radius R_C . For XTE J1751–305 we have $R_C = (GM/\Omega_S^2)^{1/3} = 26.1 m^{1/3}$ km, where M is the mass and Ω_S is the angular rotational velocity of the neutron star. The use of such a parameter is particularly suited for an accreting pulsar, as it has to be $R_{NS}/R_C < \xi(t) < 1$ in order for pulsations to be visible at a certain time t . The lower constraint is an obvious consequence of the interpretation of coherent pulsations as due to funnelling to the magnetic poles of the accreted matter, while the upper limit is due to the centrifugal inhibi-

tion of efficient accretion of matter onto the NS when the NS-magnetosphere system rotates faster than matter at the inner boundary of the disc. Expressing these boundaries in terms of m and R_6 , the radius R of the NS in units of 10^6 cm, one obtains for XTE J1751–305, $0.38R_6m^{-1/3} < \xi < 1$, which allows the definition of a range of possible accretion rates at $t = \bar{T}$, by their substitution in Eq.(5):

$$(30 \pm 6)I_{45}m^{-2/3} < \dot{M}_{10}(T_0) < (48 \pm 9)I_{45}R_6^{-1/2}m^{-1/2} \quad (6)$$

where \dot{M}_{10} is the mass accretion rate in units of $10^{-10} M_{\odot}/\text{yr}$.

This estimate of the mass accretion rate can be expressed in terms of X-ray luminosity via the usual relation $L_X = \epsilon GM\dot{M}/R_{NS}$, where $\epsilon \simeq 1$ is the rate of conversion of gravitational energy released in accretion to observable X-ray luminosity. This allows to make a comparison of the dynamical estimate of the accretion luminosity we derived from timing analysis with the one obtained by spectral modelling of the observed X-ray flux, which is obviously dependent on the source distance. By considering the expression given by GP for the bolometric luminosity, $L_X(\bar{T})$, one obtains for the distance d of XTE J1751–305:

$$d = 8.2 I_{45}^{1/2} m^{1/6} R_6^{-1/2} \epsilon^{1/2} \xi^{-1/4} \text{kpc} \quad (7)$$

Considering a moderately stiff EoS for an $m = 1.4$ NS, such as the FPS, one has for a compact object spinning at the rate measured for XTE J1751–305 $I_{45} = 1.24$ and $R_6 = 1.11$ (see e.g. Cook, Shapiro & Teukolsky 1994). It is then possible to find a range for the distance d of XTE J1751–305, $9.1 \text{kpc} \lesssim d \epsilon^{-1/2} \lesssim 11.6 \text{kpc}$.

XTE J1751–305 is located only 2° away from the Galactic Centre, so that a distance higher than 8.5 kpc would be highly improbable, if the source shows significant emission at energies of the order of ~ 1 keV (GP estimated $N_H \sim 10^{22} \text{cm}^{-2}$). However, the discrepancy between our lower limit on the distance, 9.1 kpc, and the one implied by this constraint is not large, especially considering the relatively large uncertainties underlying the simple arguments which led to our distance determination, and the assumptions made on the torque model and on the NS structure. Moreover we recall that, because of the uncertainty in the source position, the estimate of $\dot{\nu}(\bar{T})$ we used to get a dynamical estimate of the mass accretion rate is affected by a systematic error, which can in principle decrease our estimate of the distance below 8.5 kpc. M02 estimated a lower limit on the distance of 7 kpc based on indirect arguments, and our comparison between the observed $\dot{\nu}$ and the measured X-ray flux strongly supports the hypothesis that the source is close to the Galactic Centre.

Nevertheless, we can argue that the limits on the distance we find above may be overestimated due to several reasons, among which, a non isotropic emission from the source or an occultation of part of the accretion luminosity. In particular, as already noticed by GP, the fact that the pulse shape shown by XTE J1751–305 is almost sinusoidal implies that only one spot is visible from our line of sight. If this had not been the case, i.e. if also an antipodal spot had intercepted our line of sight during rotation, the folded light curves should have shown a secondary maximum (or a plateau in a more extreme case), that would have required the addition of at least an harmonic to be efficiently modelled. This picture is consistent with the re-

sults of detailed 3D magnetohydrodynamics simulations of disc accretion to this kind of rotators performed by Kulkarni & Romanova (2005). We argue that mass is accreting on both the polar caps of the compact object, with a fraction of the emitted accretion luminosity being blocked by an opaque absorber (probably by the accretion disc, as the absence of a significant Compton reflection component strongly suggests $i > 60^\circ$, see GP), and re-emitted outside the considered 0.7 – 200 keV energy band (see also Burderi et al. 2007). It could be therefore the case that the value given by GP for the X-ray flux represents an underestimate of the real emission owing to the accretion of matter. This in turn would decrease our distance estimates to values in a better agreement with the constraint of the source not being farther than the Galactic Centre. Defining η as the ratio between the effective accretion luminosity and the one observed, we find lower distance estimates that would place the source not farther than the Galactic Centre for $\eta = 1.2$, and a lower limit of 6.7 kpc corresponding to $\eta = 2$, the maximum value η may reasonably attain.

It has to be highlighted that all these estimates of the source distance are derived by assuming that no negative torque is acting on the NS, due e.g. to threading of the disc by the magnetic field lines in regions where matter in the disc rotates slower than the threading field lines, as it is assumed to explain the rotational behaviour of other source of this class (see e.g. Papitto et al. 2007). If this would not have been the case, higher estimates of the mass accretion rate would be obtained, as the observed spin frequency derivative would represent the balance between a negative torque and the positive one due to accretion at R_{in} . This would straightforwardly lead to higher estimates of the distance.

4 CONCLUSIONS

We performed a detailed timing analysis upon the coherent pulsations shown by XTE J1751–305 during its 2002 outburst as observed by *RXTE*. We could detect such a signal in the period 2002 April 4–13, i.e. in all observations during which the source emitted an X-ray flux above the quiescent level.

After having corrected for the orbital effects on phase residuals, we then showed how this source joins SAX J1808.4–3658 (Burderi et al. 2006), IGR J00291+5934 (Falanga et al. 2005; Burderi et al. 2007) and XTE J1807–294 (Riggio et al. 2007) in the class of those AMSPs that exhibit a spin up in the $10^{12} - 10^{13}$ Hz/s range, with an average rate of $(3.7 \pm 1.0) \times 10^{-13}$ Hz/s.

We applied different accretion torque models to the observed phase evolution, but we did not succeed in having a significant improvement of its description with respect to a constant spin up model either when implying a dependence of the spin frequency derivative on the instantaneous accretion rate, nor when discriminating between different scenarios of interaction between the accretion disc and the rotating magnetosphere. Applying an Alfvénic torque model we derived $\dot{\nu}_0 = (5.6 \pm 1.2) \times 10^{-13}$ Hz/s for the spin frequency derivative one day after the first observation available.

The measured value of the spin frequency derivative implies a peak accretion rate of at least 15% of the Eddington limit. Such a high accretion rate indicates that XTE J1751–

305, as already noted for IGR J00291+5934 (Burderi et al. 2007), accretes matter during outbursts at a much higher rate than that usually considered typical (a few per cent of L_{Edd}) for AMSPs.

The equality between the mass accretion rate deduced from timing when a simple Alfvénic torque model is considered, and the one obtained from a spectral analysis of the X-ray emission would place the source slightly farther than the Galactic Centre ($d \gtrsim 9.1$ kpc), although timing-based determinations of the distance may be affected by the large uncertainties on the assumed torque model.

We have also discussed the possibility that the mass accretion rate is a factor between 1 and 2 higher than the one inferred by the X-ray luminosity, if the emission of the antipodal polar cap is not visible due to the occultation by a thick absorber and re-emission of this energy is out of the considered band. An occultation of the secondary cap emission is highly improbable to be due to the star itself, while it seems more probable to owe to the accretion disc, as GP stated that the absence of a significant Compton reflection in the emitted spectrum strongly indicates $i > 60^\circ$. Defining the parameter η as the fraction of the accretion luminosity effectively emitted by the NS in the 0.7 – 200 keV energy band, with respect to the one observed ($\eta = 1 \div 2$), we get a distance estimate < 8.5 kpc when $\eta \gtrsim 1.2$, while a lower limit of $\simeq 6.7$ kpc is obtained in the case $\eta = 2$.

We acknowledge the use of *RXTE* data from the *HEASARC* public archive. We also thank the anonymous reviewer for useful comments. This work was supported by the Ministero della Istruzione della Università e della Ricerca (MIUR) national program PRIN2005 2005024090_004.

REFERENCES

- Bhattacharya D., van den Heuvel E.P.J. 1991, *Phys.Rep.*, 203, 1
 Blandford R., Teukolsky S.A. 1976, *ApJ*, 205, 580
 Bradt H., Rothschild R. E., Swank J. H. 1993, *A&AS*, 97, 355
 Burderi L., Di Salvo T., Riggio A., Menna M. T., Lavagetto G., Papitto A., Iaria R., Robba N.R., Stella L., 2007, *ApJ*, 657, 961
 Burderi L., Di Salvo T., Menna M.T., Riggio A., Papitto A., 2006, *ApJ*, 653, L133
 Cook G.B., Shapiro S.L., Teukolsky S.A., 1994, *ApJ*, 424, 823
 Di Salvo T., Burderi L., Riggio A., Papitto A., Menna M.T., 2007, in Burderi L., Di Salvo T., Fiore F., Matt G., Menna M.T., eds., *Proc. The Multicolored Landscape of Compact Objects and their Explosive Origins*, AIP, Melville, NY, vol.924, p.613
 Falanga M., Kuiper L., Poutanen J., Bonning E.W., Hermsen W., Di Salvo T., Goldoni P., Goldwurm A., Shaw S.E., Stella L., 2005, *A&A*, 444, 15
 Galloway D.K., Chakrabarty D., Morgan E.H., Remillard R.A. 2002, *ApJ*, 576, L137
 Galloway D.K. 2006, in Braga J., D’Amico F., Rothschild R.E., eds, *Proc. The Transient Milky Way: A Perspective for MI-RAX*, AIP, Melville, NY, vol.804, p.50
 Galloway D.K., Morgan E.H., Krauss M.I., Kaaret P., Chakrabarty D., 2007, *ApJ*, 654, L73
 Gierlinski M., Poutanen J., 2005, *MNRAS*, 359, 1261
 Ghosh P., 1996, *ApJ*, 459, 244
 Jahoda K., et al., 1996, Siegmund O.H., Gummin M.A., eds, *Proc. SPIE Vol. 2808, EUV, X-ray, and Gamma-Ray Instrumentation for Astronomy VII*, SPIE, Washington, p.59
 Kulkarni A.K., Romanova M.M., 2005, *ApJ*, 633, 349
 Leahy D. A., Darbro W., Elsner R. F., Weisskopf M. C., Kahn S., Sutherland P. G., Grindlay J. E., 1983, 266, 160
 Markwardt C. B., Swank J. H. 2002a, *IAU Circ.* 7867
 Markwardt C. B., Swank J. H., Strohmayer T. E., in’t Zand, J. J. M., Marshall F. E., 2002b, *ApJ*, 575, L21
 Markwardt C. B., Swank J. H., Strohmayer T. E., in’t Zand, J. J. M., Marshall F. E., 2007, *ApJ*, 667, L211
 Papitto A., Di Salvo T., Burderi L., Menna M.T., Lavagetto G., Riggio A., 2007, *MNRAS*, 375, 971
 Psaltis D., Chakrabarty D., 1999, *ApJ*, 521, 332
 Rappaport S. A., Fregeau J. M., Spruit H., 2004, *ApJ*, 606, 436
 Riggio A., Di Salvo T., Burderi L., Papitto A., Menna M.T., Iaria R., Lavagetto G., 2007, *ApJ*, submitted
 Wijnands R. 2006, *Proc. AAS Meeting* 209, 208.3
 Wijnands R., & van der Klis M., 1998, *Nature*, 394, 344